17th World Conference on Earthquake Engineering, 17WCEE
Sendai, Japan - September 13th to 18th 2020

SEISMIC EVALUATION OF SETBACK BUILDINGS

J.L. Lin [1], C.C. Tsaur [2], K.C. Tsai[3]

[1] *Research Fellow, National Center for Research on Earthquake Engineering, jllin@ncree.narl.org.tw*
[2] *Former Graduate Student, Department of Civil Engineering, National Taiwan University, r00521203@ntu.edu.tw*
[3]*Professor, Department of Civil Engineering, National Taiwan University, kctsai@ntu.edu.tw*

Abstract

Vertically irregular buildings with strong or stiff-and-strong lower stories such as setback buildings are common in engineering practice. This study proposes a seismic evaluation method for setback buildings. The conventional single-degree-of-freedom (SDOF) modal equations of motion for vertically irregular buildings with strong or stiff-and-strong lower stories are decomposed into two-degree-of-freedom (2DOF) modal equations of motion. In addition to the 2DOF modal equations of motion, the two pushover curves simultaneously obtained from the *n*-th modal pushover analysis were used together to construct the *n*-th 2DOF modal system for the target buildings. One of the two pushover curves represents the relationship between the top displacement of the upper-structure and the base shear. The other represents the relationship between the top displacement of the base-structure and the base shear. The two pushover curves presented in the acceleration–displacement–response spectra format fully overlap each other as the building remains elastic, whereas the two curves bifurcate after the building yields. This study showed that the 2DOF modal system is identical to the SDOF modal system for elastic buildings with the specific vertical irregularities. In addition, it was found that the more inelastic excursions a building with the specific vertical irregularities experiences, the less effective using the SDOF modal system to simulate the distinct modal responses for the upper-structure and base-structure will be. The proposed 2DOF modal system precisely overcame the stated deficiency of the SDOF modal system for buildings with the specific vertical irregularities. Through incorporating the 2DOF modal systems into the uncoupled modal response history analysis, the peak inter-story drift ratios (IDR) of four 9-story and four 20-story vertically irregular buildings, which have the lower stories stronger or stiffer-and-stronger than the upper stories, were satisfactorily estimated, compared with those estimated by adopting the SDOF modal systems. The investigation results highlight that the drastic change in the peak IDRs, over the two stories where the abrupt change in strength occurs, was poorly reflected by using the SDOF modal systems. In contrast, the 2DOF modal systems adequately captured this characteristic.

Keywords: vertically irregular buildings; setback buildings; modal system; modal response history analysis

1. Introduction

Vertically irregular buildings, which may possess mass, stiffness, or strength irregularities over their heights, are very common in engineering practice. For example, setbacks in upper stories, heavy mechanical mid-stories, and elevated bottom stories usually result in vertical irregularities. Therefore, vertically irregular buildings have been the subject of a significant amount of research [1].

Chintanapakdee and Chopra [2] and Chopra and Chintanapakdee [3] evaluated the feasibility of applying the modal pushover analysis (MPA) procedure [4] to estimate the seismic demands of vertically irregular frames. They concluded that, compared to the conventional pushover analysis method, the MPA procedure generally resulted in more accurate story drift estimates for vertically irregular frames. However, for frames with a strong or stiff-and-strong first story/lower half (Fig. 1a), both the simplified methods were incapable of satisfactorily estimating the seismic demands [3]. As a result, the sophisticated nonlinear response history analysis (NRHA) was the only suggested method for evaluating the seismic demands of irregular frames with a strong or stiff-and-strong first story/lower half [2, 3]. In other words, vertically irregularly buildings with strong or stiff-and-strong lower stories are the most challenging cases for simplified seismic analysis methods. Therefore, this research aims to develop a simplified seismic analysis method suitable for vertically irregular buildings, specifically with the lower stories stronger or stiffer-and-stronger than the upper stories. With this proposed method, it is expected to extend the scope of types of vertically irregular buildings to which simplified seismic analysis methods are applicable.

Note that the essential assumptions/approximations adopted in the MPA procedure [4] are that each "vibration mode" of inelastic buildings is represented as a single-degree-of-freedom (SDOF) modal system. In addition, the MPA procedure still approximately applied the superposition of "modal responses" to inelastic buildings [4]. Nevertheless, it is natural that the generalized modal coordinate for the upper-structure, which are weak and/or soft stories shown in Fig. 1, is very likely different from that for the base-structure, which are strong and/or stiff stories shown in Fig. 1. For instance, the upper-structure exhibits large inelastic excursions, whereas the base-structure remains essentially elastic. In such a case, it appears insufficient to employ the SDOF modal responses for recovering both the seismic responses of the upper-structure and base-structure.

Therefore, this study develops two-degree-of-freedom (2DOF) modal systems instead of SDOF modal systems to characterize the distinctly different modal responses of the upper-structure and base-structure. The proposed simplified seismic analysis method involves performing the uncoupled modal response history analysis (UMRHA) [4], in which the SDOF modal systems are replaced by the proposed 2DOF modal systems. UMRHA is the counterpart of the MPA procedure. UMRHA estimates the whole response history but MPA estimates only the peak responses. This study verifies the effectiveness of the proposed method by evaluating the seismic responses of four 9-story and four 20-story vertically irregular buildings under the excitation of three ensembles of ground motion records.

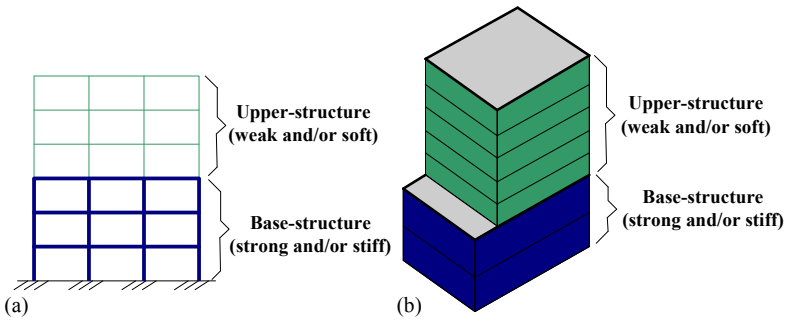

Fig. 1 – (a) A schematic drawing of a building frame with a strong and/or stiff lower half. (b) A schematic drawing of a setback building.

2. Theoretical background

Based on the approach of constructing the 2DOF modal system to represent each vibration mode of one-way asymmetric-plan buildings [5], this study further develops the 2DOF modal system for the vertically irregular buildings with strong or stiff-and-strong lower stories as follows.

2.1 Elastic properties of 2DOF modal systems

Considering an *N*-story building, whose base-structure contains the first to *j*-th stories and the upper-structure contains the (*j* + 1)-th to *N*-th stories, the equation of motion of this building is:

$$\mathbf{M}\ddot{\mathbf{u}} + \mathbf{C}\dot{\mathbf{u}} + \mathbf{K}\mathbf{u} = -\mathbf{M}\boldsymbol{\iota}\ddot{u}_g \tag{1a}$$

where:

$$\mathbf{u} = \begin{bmatrix} \mathbf{u}_p \\ \mathbf{u}_b \end{bmatrix}_{N\times 1}, \quad \mathbf{M} = \begin{bmatrix} \mathbf{m}_p & \mathbf{0} \\ \mathbf{0} & \mathbf{m}_b \end{bmatrix}_{N\times N}, \quad \mathbf{C} = \begin{bmatrix} \mathbf{c}_{pp} & \mathbf{c}_{pb} \\ \mathbf{c}_{bp} & \mathbf{c}_{bb} \end{bmatrix}_{N\times N}, \quad \mathbf{K} = \begin{bmatrix} \mathbf{k}_{pp} & \mathbf{k}_{pb} \\ \mathbf{k}_{bp} & \mathbf{k}_{bb} \end{bmatrix}_{N\times N} \tag{1b}$$

and $\boldsymbol{\iota}$ and $\ddot{u}_g$ are the influence vector and the ground acceleration record, respectively. In Eq. 1b, the subscripts *p* and *b* denote the corresponding quantities belonging to the upper-structure and base-structure, respectively. Each floor of the considered building is assumed to be a rigid floor diaphragm with only one translational degree of freedom. Therefore, $\mathbf{u}_p$ and $\mathbf{u}_b$ are $(N - j) \times 1$ and $j \times 1$ column vectors, respectively, and the sizes of the sub-matrices shown in Eq. 1b are determined accordingly. The earthquake load, *i.e.*, the right-hand side of Eq. 1a, can be expressed as [6]:

$$-\mathbf{M}\boldsymbol{\iota}\ddot{u}_g = -\sum_{n=1}^{N}\mathbf{s}_n\ddot{u}_g = -\sum_{n=1}^{N}\Gamma_n\mathbf{M}\boldsymbol{\varphi}_n\ddot{u}_g \tag{2}$$

where Γ_n and $\boldsymbol{\varphi}_n$ are the *n*-th modal participation factor and the mode shape, respectively, and $\mathbf{s}_n$ is the *n*-th modal inertia force vector, which is equal to $\Gamma_n\mathbf{M}\boldsymbol{\varphi}_n$. When the building is subjected to $\mathbf{s}_n\ddot{u}_g$, only the *n*-th modal displacement vector, denoted as $\mathbf{u}_n$, is excited. Therefore, Eq. 1a can be expressed as:

$$\mathbf{M}\ddot{\mathbf{u}}_n + \mathbf{C}\dot{\mathbf{u}}_n + \mathbf{K}\mathbf{u}_n = -\mathbf{s}_n\ddot{u}_g \tag{3a}$$

where:

$$\mathbf{u}_n = \Gamma_n\boldsymbol{\varphi}_n D_n = \Gamma_n\begin{bmatrix} \boldsymbol{\varphi}_{pn} \\ \boldsymbol{\varphi}_{bn} \end{bmatrix} D_n \tag{3b}$$

and D_n is the *n*-th generalized modal coordinate. In the UMRHA [4], $D_n(t)$ (Eq. 3b) is obtained from solving the *n*-th SDOF modal equation of motion. The relationship between the restoring force and the generalized modal coordinate of the *n*-th SDOF modal system is represented as a bilinear curve, which is idealized from the *n*-th modal pushover curve of the target building presented in the acceleration–displacement–response spectra (ADRS) format. The *n*-th modal pushover curve is the force vs. displacement relationship of the target building pushed using $\mathbf{s}_n$. The total displacement history of the target building, $\mathbf{u}(t)$, is equal to the arithmetic summation of $\mathbf{u}_n(t)$, $n = 1 \sim N$. While computing $\mathbf{u}_n(t)$, the elastic mode shape $\boldsymbol{\varphi}_n$ and the elastic modal participation factor Γ_n are used in Eq. 3b, irrespective of elastic or inelastic modal responses. The basic assumptions or approximations adopted in the UMRHA still exist in the proposed approach except the single generalized modal coordinate is replaced by the two generalized modal coordinates. This study thus rearranges Eq. 3b as:

$$\mathbf{u}_n = \Gamma_n\begin{bmatrix} \boldsymbol{\varphi}_{pn} & \mathbf{0}_{pb} \\ \mathbf{0}_{bp} & \boldsymbol{\varphi}_{bn} \end{bmatrix}_{N\times 2}\begin{bmatrix} D_{pn} \\ D_{bn} \end{bmatrix}_{2\times 1} = \Gamma_n\boldsymbol{\Phi}_n\mathbf{D}_n \tag{4a}$$

where:

$$\boldsymbol{\Phi}_n = \begin{bmatrix} \boldsymbol{\varphi}_{pn} & \mathbf{0}_{pb} \\ \mathbf{0}_{bp} & \boldsymbol{\varphi}_{bn} \end{bmatrix}_{N\times 2}, \quad \mathbf{D}_n = \begin{bmatrix} D_{pn} \\ D_{bn} \end{bmatrix}_{2\times 1} \tag{4b}$$

and $\mathbf{0}_{pb}$ and $\mathbf{0}_{bp}$ are the $(N-j) \times 1$ and $j \times 1$ zero vectors, respectively. Substituting Eq. 4a into Eq. 3a and pre-multiplying both sides of Eq. 3a by $\boldsymbol{\Phi}_n^T$ result in:

$$\mathbf{M}_n \ddot{\mathbf{D}}_n + \mathbf{C}_n \dot{\mathbf{D}}_n + \mathbf{K}_n \mathbf{D}_n = -\mathbf{M}_n \mathbf{1} \ddot{u}_g \tag{5a}$$

where:

$$\mathbf{M}_n = \begin{bmatrix} \boldsymbol{\varphi}_{pn}^T \mathbf{m}_p \boldsymbol{\varphi}_{pn} & 0 \\ 0 & \boldsymbol{\varphi}_{bn}^T \mathbf{m}_b \boldsymbol{\varphi}_{bn} \end{bmatrix}_{2\times 2}, \quad \mathbf{C}_n = \begin{bmatrix} \boldsymbol{\varphi}_{pn}^T \mathbf{c}_{pp} \boldsymbol{\varphi}_{pn} & \boldsymbol{\varphi}_{pn}^T \mathbf{c}_{pb} \boldsymbol{\varphi}_{bn} \\ \boldsymbol{\varphi}_{bn}^T \mathbf{c}_{bp} \boldsymbol{\varphi}_{pn} & \boldsymbol{\varphi}_{bn}^T \mathbf{c}_{bb} \boldsymbol{\varphi}_{bn} \end{bmatrix}_{2\times 2}, \quad \mathbf{K}_n = \begin{bmatrix} \boldsymbol{\varphi}_{pn}^T \mathbf{k}_{pp} \boldsymbol{\varphi}_{pn} & \boldsymbol{\varphi}_{pn}^T \mathbf{k}_{pb} \boldsymbol{\varphi}_{bn} \\ \boldsymbol{\varphi}_{bn}^T \mathbf{k}_{bp} \boldsymbol{\varphi}_{pn} & \boldsymbol{\varphi}_{bn}^T \mathbf{k}_{bb} \boldsymbol{\varphi}_{bn} \end{bmatrix}_{2\times 2} \tag{5b}$$

and $\mathbf{1} = [1\ 1]^T$. Eq. 5 is the *n*-th 2DOF modal equation of motion for the considered building.

The mechanical analogy model corresponding to Eq. 5 is in demand for nonlinear modal response history analysis. Fig. 2a shows the proposed physical model of the *n*-th 2DOF modal system, whose vibration is represented as the *n*-th 2DOF modal equation of motion (Eq. 5). The *n*-th 2DOF modal system consists of two rigid bars with lengths equal to l_{pn} and l_{bn}, respectively (Fig. 2a). Two lumped masses, denoted m_{pn} and m_{bn}, are located at the tops of the upper and lower rigid bars, respectively. The upper rigid bar is pin-connected to the lower rigid bar by a rotational spring with rotational stiffness k_{pn}. Similarly, the lower rigid bar is pin-connected to the ground by a rotational spring with rotational stiffness k_{bn} (Fig. 2a). For the simple structural model shown in Fig. 2a, its corresponding mass matrix $\tilde{\mathbf{M}}_n$, stiffness matrix $\tilde{\mathbf{K}}_n$, and displacement vector $\tilde{\mathbf{D}}_n$, which is defined as the two translations at the two lumped masses, are formulated as:

$$\tilde{\mathbf{D}}_n = \begin{bmatrix} \tilde{D}_{pn} \\ \tilde{D}_{bn} \end{bmatrix}_{2\times 1}, \quad \tilde{\mathbf{M}}_n = \begin{bmatrix} m_{pn} & 0 \\ 0 & m_{bn} \end{bmatrix}_{2\times 2}, \quad \tilde{\mathbf{K}}_n = \begin{bmatrix} \dfrac{k_{pn}}{l_{pn}^2} & \dfrac{-k_{pn}}{l_{pn}^2}\left(1+\dfrac{l_{pn}}{l_{bn}}\right) \\ \dfrac{-k_{pn}}{l_{pn}^2}\left(1+\dfrac{l_{pn}}{l_{bn}}\right) & \dfrac{k_{pn}}{l_{pn}^2}\left(1+\dfrac{l_{pn}}{l_{bn}}\right)^2 + \dfrac{k_{bn}}{l_{bn}^2} \end{bmatrix}_{2\times 2} \tag{6}$$

By setting $\tilde{\mathbf{D}}_n = \mathbf{D}_n$, $\tilde{\mathbf{M}}_n = \mathbf{M}_n$, $\tilde{\mathbf{K}}_n = \mathbf{K}_n$, and $l_{pn} = 1$, all the elastic properties of the *n*-th 2DOF modal system are obtained as:

$$\begin{aligned} m_{pn} &= \boldsymbol{\varphi}_{pn}^T \mathbf{m}_p \boldsymbol{\varphi}_{pn}, \quad m_{bn} = \boldsymbol{\varphi}_{bn}^T \mathbf{m}_b \boldsymbol{\varphi}_{bn}, \quad l_{bn} = -\left(\frac{\boldsymbol{\varphi}_{pn}^T \mathbf{k}_{pb} \boldsymbol{\varphi}_{bn}}{\boldsymbol{\varphi}_{pn}^T \mathbf{k}_{pp} \boldsymbol{\varphi}_{pn}} + 1 \right)^{-1} \\ k_{pn} &= \boldsymbol{\varphi}_{pn}^T \mathbf{k}_{pp} \boldsymbol{\varphi}_{pn}, \quad k_{bn} = l_{bn}^2 \left(\boldsymbol{\varphi}_{bn}^T \mathbf{k}_{bb} \boldsymbol{\varphi}_{bn} - \frac{\left(\boldsymbol{\varphi}_{pn}^T \mathbf{k}_{pb} \boldsymbol{\varphi}_{bn} \right)^2}{\boldsymbol{\varphi}_{pn}^T \mathbf{k}_{pp} \boldsymbol{\varphi}_{pn}} \right) \end{aligned} \tag{7}$$

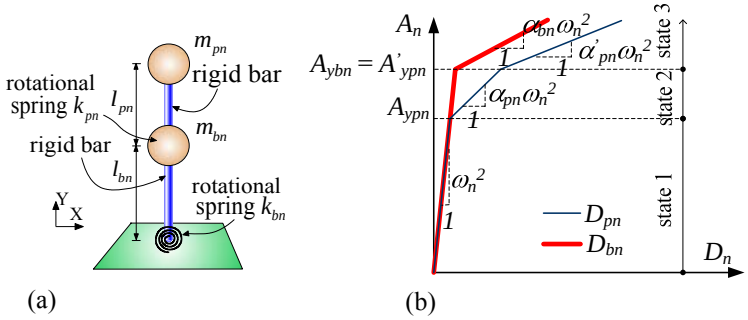

Fig. 2 – (a) The *n*-th 2DOF modal system. (b) The pushover curves A_n vs. D_{pn} and A_n vs. D_{bn} relationships.

2.2 Inelastic properties of 2DOF modal systems

When a building with the specific vertical irregularities is pushed by the *n*-th modal inertia force $\mathbf{s}_n$, it can obtain the pushover curve, which represents the relationship between the base shear, denoted V_{bn}, and the displacement at the top of upper-structure, denoted $u_{n,tp}$. It can simultaneously obtain the other pushover curve, which represents the relationship between the base shear V_{bn} and the displacement at the top of the base-structure, denoted $u_{n,tb}$. The two pushover curves are transformed into the ADRS format by means of the following equations:

$$D_{pn} = \frac{u_{n,tp}}{\Gamma_n \phi_{n,tp}}, \quad D_{bn} = \frac{u_{n,tb}}{\Gamma_n \phi_{n,tb}}, \quad A_n = \frac{V_{bn}}{\Gamma_n^2 M_n} \tag{8}$$

, in which $\phi_{n,tp}$ and $\phi_{n,tb}$ are the components of the *n*-th mode shape at the tops of the upper-structure and the base-structure, respectively. Additionally, M_n is the modal mass, which is equal to $\boldsymbol{\varphi}_n^T \mathbf{M} \boldsymbol{\varphi}_n$. The two pushover curves are approximately represented as two polygonal lines (Fig. 2b). When the building completely remains elastic (*i.e.*, state 1 shown in Fig. 2b), the two pushover curves overlap with a slope equal to ω_n^2, in which ω_n is the circular frequency of the *n*-th vibration mode of the building. When the upper-structure yields and the base-structure remains elastic (*i.e.*, state 2 shown in Fig. 2b), the slopes of the two pushover curves A_n—D_{pn} and A_n—D_{bn} are $\alpha_{pn}\omega_n^2$ and ω_n^2, respectively. The ordinate of the inflection point of the pushover curve A_n—D_{pn} is denoted as A_{ypn} (Fig. 2b), which represents the yielding acceleration of the upper-structure. Furthermore, when both the upper-structure and the base-structure become inelastic (*i.e.*, state 3 shown in Fig. 2b), the slopes of the two pushover curves A_n—D_{pn} and A_n—D_{bn} are $\alpha'_{pn}\omega_n^2$ and $\alpha_{bn}\omega_n^2$. The ordinate of the inflection point of the pushover curve A_n—D_{bn} is denoted as A_{ybn} (Fig. 2b), which represents the yielding acceleration of the base-structure. A_{ybn} also represents the ordinate of the second inflection point of the pushover curve A_n—D_{pn}, denoted as A'_{ypn} (*i.e.*, $A'_{ypn} = A_{ybn}$).

Likewise, two pushover curves are available when the *n*-th 2DOF modal system (Fig. 2a) is pushed by its active modal inertia force. One of the two pushover curve represents the relationship between the base shear and the displacement at the top of the upper rigid bar. The other pushover curve represents the relationship between the base shear and the displacement at the top of the lower rigid bar. The two pushover curves obtained from the *n*-th 2DOF modal system presented in the ADRS format are expected to be the same as those obtained from the building model pushed by its *n*-th modal inertia force $\mathbf{s}_n$. In addition, when the *n*-th 2DOF modal system (Fig. 2a) is pushed by its active modal inertia force, three states are considered. In state 1, both the rotational springs of the 2DOF modal system remain elastic. In state 2, the lower rotational spring remains elastic, whereas the upper rotational spring yields, which has a stiffness k'_{pn}. In state 3, the lower rotational spring yields, which has a stiffness k'_{bn}, and the stiffness of the upper rotational spring becomes k''_{pn}. Therefore, the lower spring is simulated as a bilinear rotational spring, whose yielding moment is denoted as M_{ybn}. In addition, the upper spring is simulated as a trilinear rotational spring, whose

moments corresponding to the first and second inflection points are denoted as M_{ypn} and M'_{ypn}, respectively. The values of the six parameters k'_{pn}, k''_{pn}, k'_{bn}, M_{ypn}, M'_{ypn}, and M_{ybn} can be determined in terms of the six parameters α_{pn}, α'_{pn}, α_{bn}, A_{ypn}, A'_{ypn}, and A_{ybn}, whose values are available from the building's pushover curves (Fig. 2b). The six parameters k'_{pn}, k''_{pn}, k'_{bn}, M_{ypn}, M'_{ypn}, and M_{ybn} of the two rotational springs used in the *n*-th 2DOF modal system are expressed as follows:

$$k'_{pn} = \frac{m_{pn}}{\dfrac{m_{pn}}{k_{pn}} + \dfrac{\left(l_{bn}+1\right)\left(l_{bn}+m_{pn}\right)}{k_{bn}} - \dfrac{\left(l_{bn}+1\right)\left(l_{bn}+m_{pn}\right)}{k_{bn}}}$$

$$k''_{pn} = \frac{m_{pn}}{\dfrac{m_{pn}}{k_{pn}} + \dfrac{\left(l_{bn}+1\right)\left(l_{bn}+m_{pn}\right)}{k_{bn}} - \dfrac{\left(l_{bn}+1\right)\left(l_{bn}+m_{pn}\right)}{k'_{bn}}} \tag{9}$$

$$k'_{bn} = \alpha_{bn} k_{bn}, \quad M_{ypn} = A_{ypn} m_{pn}, \quad M'_{ypn} = A_{ybn} m_{pn}, \quad M_{ybn} = A_{ybn}\left[\left(1+l_{bn}\right)m_{pn} + l_{bn} m_{bn}\right]$$

The damping matrix of the 2DOF modal system is computed using Rayleigh damping with the assumption that the damping ratios of the two sub-modes are equal to the damping ratio of the *n*-th vibration mode of the building. The elastic properties (Eq. 7) and the inelastic properties (Eq. 9) of the 2DOF modal system are now completely determined. That is to say, the construction of the *n*-th 2DOF modal system is complete.

2.3 Procedures of the proposed simplified seismic analysis method

The procedures of the proposed simplified seismic analysis method are the same as those of UMRHA [4]. The essential difference between the proposed method and UMRHA is that the SDOF modal systems used in UMRHA are replaced by 2DOF modal systems in the proposed method. Therefore, to clarify the different numbers of degrees of freedom, this study designates the proposed method and UMRHA as 2DM and SDM, respectively. The procedures of the proposed simplified seismic analysis method are as follows:

Step 1: Perform eigenvalue analysis of the building model. The mode shapes, vibration frequencies, and damping ratios of all vibration modes are obtained.

Step 2: Set n = 1. In addition, the number of concerned vibration modes is defined as s. For most building structures, s = 3 is sufficient. That is to say, considering the first three vibration modes in the direction of applied ground motions is sufficient for performing modal response history analysis.

Step 3: Using Eq. 7, compute the elastic properties of the *n*-th 2DOF modal system. Note that Eq. 7 requires $\mathbf{k}_{pp}$, $\mathbf{k}_{bb}$, and $\mathbf{k}_{pb}$, which are the sub-matrices of the stiffness matrix, $\mathbf{K}$, of the building (Eq. 1b). If $\mathbf{k}_{pp}$, $\mathbf{k}_{bb}$, and $\mathbf{k}_{pb}$ are not accessible from the structural analysis program, the stiffness matrix $\mathbf{K}$ can be computed as $\left(\mathbf{\Phi}^T\right)^{-1}\mathbf{\Lambda}\mathbf{\Phi}^T\mathbf{M}\mathbf{\Phi}\mathbf{\Phi}^{-1}$, where $\mathbf{\Lambda}$ is the diagonal matrix with diagonal elements ω_1^2, ω_2^2,…, ω_N^2, and $\mathbf{\Phi}$ is the matrix of mode shapes, i.e. $\left[\boldsymbol{\varphi}_1 \quad \boldsymbol{\varphi}_2 \quad \cdots \quad \boldsymbol{\varphi}_N\right]$. Once the stiffness matrix $\mathbf{K}$ is obtained, the sub-matrices $\mathbf{k}_{pp}$, $\mathbf{k}_{bb}$, and $\mathbf{k}_{pb}$ can be conveniently identified from $\mathbf{K}$ because each mode shape is treated as a two-part vector, i.e., one part for the upper-structure and the other for the base-structure.

Step 4: Push the target building model with the *n*-th modal inertia force $\mathbf{s}_n$. Through Eq. 8, the two pushover curves presented in the ADRS format (*i.e.*, A_n vs. D_{pn} and A_n vs. D_{bn} relationships) are obtained accordingly.

Step 5: Idealize the two pushover curves A_n vs. D_{pn} and A_n vs. D_{bn} relationships as trilinear and bilinear curves, respectively. First, this study uses the equal-area principle to determine the inflection point of the pushover curve A_n vs. D_{bn} relationship. Second, the second inflection point of the trilinear curve A_n vs. D_{pn} relationship is the point of the original curve with the ordinate equal to A_{ybn} (*i.e.*, $A'_{ypn} = A_{ybn}$), which is the ordinate of the inflection point of the bilinear pushover curve A_n vs. D_{bn} relationship. Third, the first inflection point of the trilinear curve A_n vs. D_{pn} relationship is again determined using the equal-area principle. That is to say, the area enclosed by the trilinear curve is equal to that enclosed by the original curve. The values of α_{pn}, α'_{pn}, α_{bn}, A_{ypn}, A'_{ypn}, and A_{ybn} are obtained from the two idealized curves (Fig. 2b).

Step 6: Using Eq. 9, compute the inelastic properties of the n-th 2DOF modal system, *i.e.*, k'_{pn}, k''_{pn}, k'_{bn}, M_{ypn}, M'_{ypn}, and M_{ybn}. The n-th 2DOF modal system is now constructed.

Step 7: Perform inelastic dynamic analysis of the n-th 2DOF modal system subjected to the selected ground motion records. The response histories at the two lumped masses are obtained (*i.e.*, $D_{pn}(t)$ and $D_{bn}(t)$).

Step 8: With $D_{pn}(t)$ and $D_{bn}(t)$, compute the inter-story drift ratio of the i-th story of the upper-structure contributed by the n-th vibration mode, denoted as $\theta_{n,i}$, as:

$$\theta_{n,i}(t) = \frac{\Gamma_n\left(\varphi_{n,i} - \varphi_{n,i-1}\right)\delta_n(t)}{h_i}, \quad \delta_n(t) = \frac{\Gamma_n\varphi_{n,tp}D_{pn}(t) - \Gamma_n\varphi_{n,tb}D_{bn}(t)}{\Gamma_n\left(\varphi_{n,tp} - \varphi_{n,tb}\right)} \tag{10a}$$

, in which h_i is the i-th story height. In addition, compute the inter-story drift ratio of the k-th story of the base-structure contributed by the n-th vibration mode, denoted as $\theta_{n,k}$, as:

$$\theta_{n,k}(t) = \begin{cases} \dfrac{\Gamma_n\left(\varphi_{n,k} - \varphi_{n,k-1}\right)D_{bn}(t)}{h_k}, & k \neq 1 \\ \dfrac{\Gamma_n\varphi_{n,k}D_{bn}(t)}{h_1}, & k = 1 \end{cases} \tag{10b}$$

, in which h_k is the k-th story height. Therefore, the inter-story drift ratios of the building contributed from the n-th vibration mode, denoted as $\boldsymbol{\theta}_n(t)$, are obtained. Note that δ_n (Eq. 10a) is the upper-structure's drift relative to the base-structure presented in the modal space. With the same manner used in Eq. 10a, D_{bn} could be regarded as the base-structure's drift relative to the fixed ground presented in the modal space (i.e., $D_{bn} = \dfrac{\Gamma_n\varphi_{n,tb}D_{bn}(t) - 0}{\Gamma_n\left(\varphi_{n,tb} - 0\right)}$). That is to say, the inter-story drift ratios are computed based on the upper-structure's and the base-structure's relative drifts (Eqs. 10a and 10b).

Step 9: Set $n = n + 1$. If $n \leq s$, then repeat Steps 3 to 8. Otherwise, go to Step 10.

Step 10: Compute the time-histories of the building's inter-story drift ratios as $\boldsymbol{\theta}(t) \approx \sum_{n=1}^{s}\boldsymbol{\theta}_n(t)$. Then stop the analysis procedures.

3. Numerical verification

3.1 Building models and ground motion records

According to the UBC [7] provisions, the SAC steel research project [8] designed one 9-story and one 20-story steel perimeter moment-resisting frame buildings located in Los Angeles. The two buildings were designed as typical office buildings standing on stiff soil. This current study takes two plane frames out of the two buildings for use as reference regular frames, designated as SAC9 and SAC20, respectively (Fig. 3). All floors of SAC9 and SAC20 are simulated as rigid diaphragms. All of the beam and column members are simulated using the beam–column element of the structural analysis program PISA3D [9]. The beam–column elements allow plastic hinges to be formed at both ends of each member. The materials used in the beams and columns are Dual A36 Gr. 50 steel and A572 Gr. 50 steel, respectively. The yield strengths of the two steel materials used in the beams and columns are 340 and 345 MPa, respectively. The simulated stress–strain relationships of the steel materials are bilinear, have a Young's modulus of $E = 2.0 \times 10^5$ MPa, and a 3% post-yielding stiffness ratio.

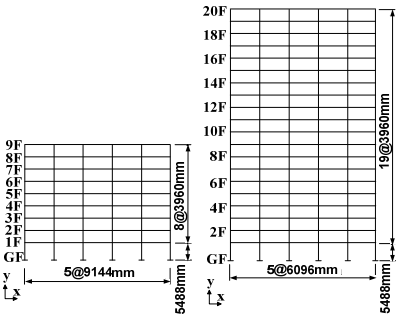

Fig. 3 – The reference regular frames SAC9 and SAC20.

The vertically irregular frames are varied from SAC9 and SAC20 by altering only the strengths of the stories or both the stiffnesses and strengths of the stories. When altering the strengths of certain stories, denoted as 'S', the yielding strengths of the materials for all beams and columns of the stories are reduced to half of their original values. When altering the strengths and stiffnesses of certain stories, denoted as 'SK', both the yielding strengths and Young's modulus of the materials for all beams and columns of the stories are reduced to half of their original values.

In addition, this study considers two cases with different numbers of stories with altered strength and/or stiffness. In the first case, the stories of the upper half of the building are altered. In the second case, all the stories except the first story are altered. Therefore, there are four vertically irregular frames varied from SAC9, denoted as SAC9S2, SAC9S5, SAC9SK2, and SAC9SK5. The last number denotes the initial story that is altered, and the stories above this are also altered. For instance, the last number '2' (or '5') denotes that the 2nd (or the 5th) story and the stories above the 2nd (or the 5th) story are altered. Likewise, there are four vertically irregular frames varied from SAC20, denoted as SAC20S2, SAC20S11, SAC20SK2, and SAC20SK11. For instance, SAC20SK2 represents a vertically irregular building varied from SAC20, in which both the strength (*i.e.*, 'S') and stiffness (*i.e.*, 'K') of the 2nd and higher stories are reduced to half of those of SAC20.

The three ensembles of ground motion records used in the SAC steel research project for buildings located in Los Angeles are also used in this study. The three ensembles of ground motion records, each of which consists of twenty ground motion records, are designated as the 50/50, 10/50, and 2/50 sets. The 50/50 set, which includes the ground motion records LA41 to LA60, represents the seismic hazard of a 72-year return period at the building site. The 10/50 set, which includes the ground motion records LA1 to LA20, represents the seismic hazard of a 475-year return period at the building site. The 2/50 set, which includes the ground motion records LA21 to LA40, represents the seismic hazard of a 2475-year return period at the building site. The details of the sixty ground motion records (*i.e.*, LA1 to LA60) are available in the associated SAC report [8]. All the ground motion records are applied in the *x*-direction.

3.2 2DOF modal systems

By performing eigenvalue analyses, the vibration periods and accumulative modal participation mass ratios of the first three vibration modes for each of the eight example frames are listed in Table 1. Note that the alteration of story strength does not change the elastic stiffness of the buildings. Therefore, the modal properties, including the modal vibration periods and mode shapes, of SAC9S2 and SAC9S5 are identical to those of the original regular frame (*i.e.*, SAC9). Likewise, the modal properties of SAC20S2 and SAC20S11 are identical to those of SAC20. The accumulative modal participation mass ratio of the first three vibration modes is over 90% (Table 1), which indicates that considering the first three vibration modes is sufficient for analyzing these example frames through modal response history analysis.

Table 1 – The vibration periods and accumulative modal participation mass ratios of the example frames.

Frame	T_1 (sec)	T_2 (sec)	T_3 (sec)	$\sum_{i=1}^{3}\Gamma_i^2 M_i / \sum_{i=1}^{N}\Gamma_i^2 M_i$
SAC9S2	2.28	0.84	0.47	0.97
SAC9S5	2.28	0.84	0.47	0.97
SAC9SK2	2.99	1.09	0.60	0.95
SAC9SK5	2.62	1.03	0.57	0.96
SAC20S2	3.84	1.33	0.76	0.95
SAC20S11	3.84	1.33	0.76	0.95
SAC20SK2	5.18	1.78	1.00	0.93
SAC20SK11	4.22	1.61	0.92	0.93

By separately pushing the eight vertically irregular frames with their own modal inertia forces $\mathbf{s}_n$, where n = 1–3, the pushover curves A_n vs. D_{pn} and A_n vs. D_{bn} relationships are obtained, as shown in Fig. 4, which have been transformed into the ADRS format using Eq. 8. It is found that the two pushover curves (*i.e.*, the A_n—D_{pn} and A_n—D_{bn} curves) overlap when the frames remain elastic, whereas these two curves bifurcate as the frames become inelastic. Because the unit of measurement of the ordinates of Fig. 4 is the acceleration due to gravity, the slopes of the elastic segments of the curves shown in Fig. 4 multiplied by 9.81 are equal to ω_n^2 ($= 4\pi^2/T_n^2$), where n = 1–3 and T_n is the n-th vibration period shown in Table 1. This implies that the elastic 2DOF modal system, in which $D_{pn} = D_{bn}$, is identical to the corresponding elastic SDOF modal system. In addition, Fig. 4 indicates that the difference between D_{pn} and D_{bn}, where n = 1 to 3, increases as the inelastic excursion increases. That is to say, it becomes insufficient to use SDOF modal systems for estimating the modal responses of the building with substantial inelasticity.

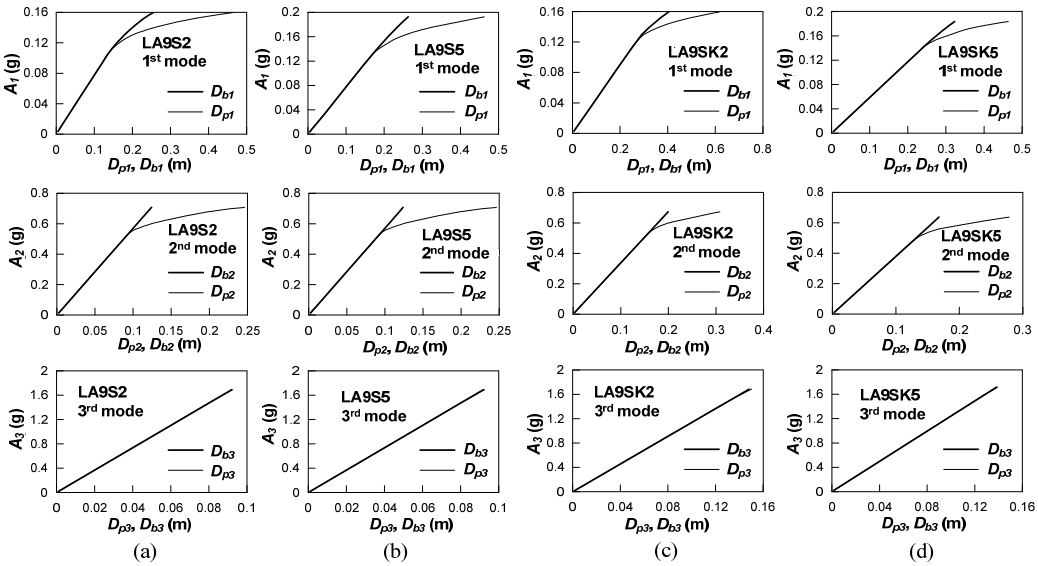

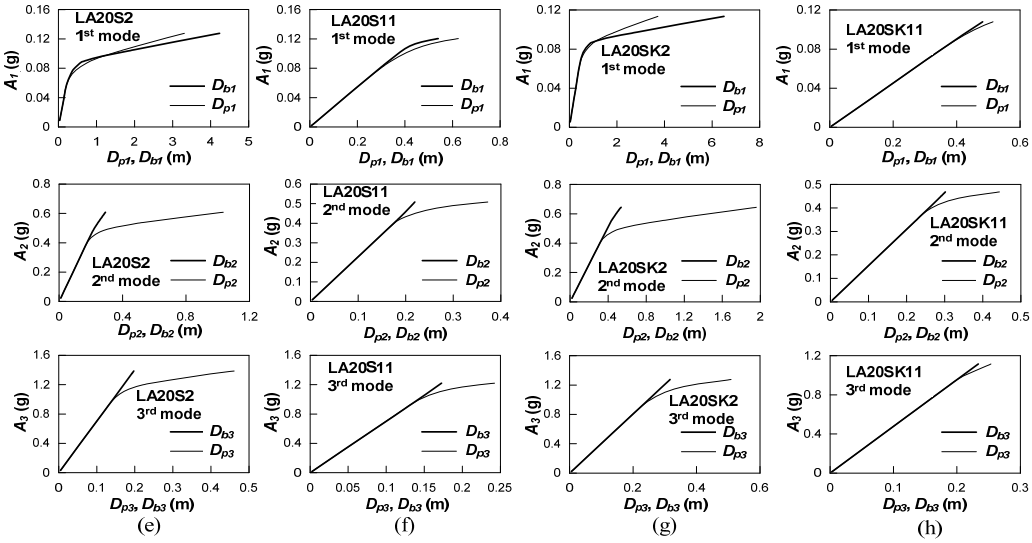

Fig. 4 – The A_n vs. D_{pn} and A_n vs. D_{bn} relationships of the first three vibration modes of (a) SAC9S2, (b) SAC9S5, (c) SAC9SK2, (d) SAC9SK5, (e) SAC20S2, (f) SAC20S11, (g) SAC20SK2, and (h) SAC20SK11.

3.3 Analysis results

The left and right two columns of Fig. 5 respectively show the peak IDRs of SAC9S5 and SAC20S11 subjected to LA3, LA5, LA6, and LA7. In Fig. 5, only the first three vibration modes are considered by the 2DM and SDM. Because SAC20S11 remains elastic while subjected to LA7, the corresponding peak IDRs obtained from the 2DM are the same as those obtained from the SDM. Fig. 5 shows that the exact peak IDRs obtained from the FEM drastically increase from the top story of the base-structure (*i.e.*, the 4th/10th story for SAC9S5/SAC20S11) to the bottom story of the upper-structure (*i.e.*, the 5th/11th story for SAC9S5/SAC20S11). This characterization of the drastic change in the peak IDRs at adjacent stories, which separately belong to the base-structure and the upper-structure, is better captured using the 2DM in comparison with the SDM (Fig. 5). In addition, the peak IDRs estimated by the SDM, which do not reflect the abovementioned drastic change over the building height, are generally in the middle of the peak IDRs of the base-structure and those of the upper-structure. As a result, the SDM generally overestimates and underestimates the peak IDRs of the base-structure and the upper-structure, respectively (Fig. 5). In contrast, the 2DM, which uses two modal coordinates (*i.e.*, D_{pn} and D_{bn}) in each vibration mode to respectively describe the distinct modal responses of the upper-structures and base-structures of the building frames, satisfactorily improves the estimated IDRs (Fig. 5).

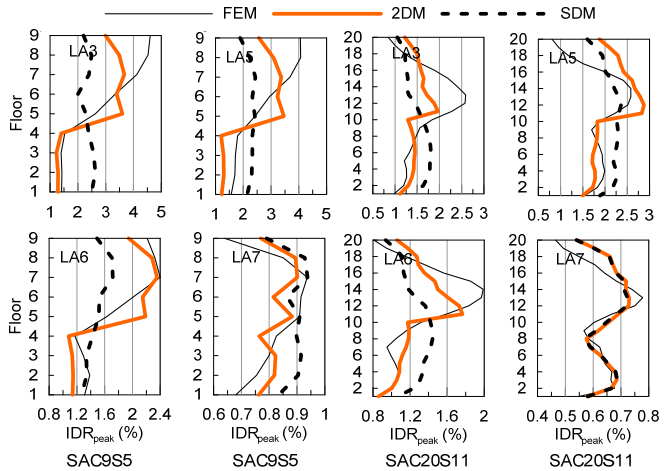

Fig. 5 – The plots in the left two columns show the peak IDRs of SAC9S5 subjected to LA3, LA5, LA6, and LA7. The plots on the right two columns show the peak IDRs of SAC20S11 subjected to LA3, LA5, LA6, and LA7.

Figs. 6a and 6b show the hysteretic loops of the first three 2DOF modal systems for SAC9S5 subjected to LA3 and LA26, respectively, compared with those of the corresponding SDOF modal systems. Fig. 6a shows that the upper springs are significantly inelastic and the lower springs are essentially elastic. Nevertheless, the single springs adopted in the SDM for the first two vibration modes are slightly inelastic, in which the inelastic excursions are not as significant as those of the upper springs incorporated in the 2DOF modal systems. In addition, the single spring incorporated in the SDOF modal system for the 3rd vibration mode is elastic, which is the same as the two springs incorporated in the 2DOF modal system. In Fig. 6b, the extents of inelasticity of both the 2DOF and SDOF modal systems for the first and second vibration modes increase, compared with those shown in Fig. 6a. Nevertheless, the inelastic excursions of the single spring incorporated in the SDOF modal system are still in the middle of those of the upper and lower springs incorporated in the 2DOF modal systems. Fig. 6 clearly indicates that the upper-structure may significantly yield while the base-structure remains essentially elastic or slightly inelastic. This phenomenon is hardly reflected using the SDOF modal system, which has only one modal coordinate (*i.e.*, D_n). This may further explain the significant differences between the estimated peak IDRs obtained from the 2DM and SDM (Fig. 5).

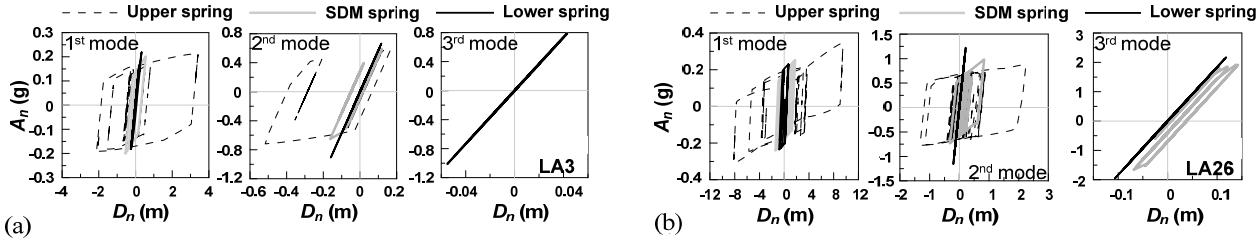

Fig. 6 – The hysteretic loops of the two rotational springs incorporated in each of the first three 2DOF modal systems for SAC9S5 subjected to (a) LA3 and (b) LA26, compared with that of the single spring incorporated in each of the first three SDOF modal systems.

The statistical results for the 9-story and 20-story buildings subjected to each of the three ensembles of ground motion records are separately processed [10]. From the statistical results, it is aware that both the SDM and the 2DM provide the predictions of the mean of the peak IDRs with more-or-less the same level of accuracy for the vertically irregular buildings with stiff-and-strong lower stories (i.e., SAC9SK2, SAC9SK5, SAC20SK2, and SAC20SK11). Although the other type of vertical irregularity (i.e., buildings with strong-only lower stories) may not be very common in reality, nonetheless, the 2DM outperforms the SDM in estimating the mean of the peak IDRs for such example buildings (i.e., SAC9S2, SAC9S5, SAC20S2, and SAC20S11). The key to this remark lies that the 2DM satisfactorily captures the drastic change of inter-story drift ratios occurred between the upper-structure and the base-structure, whereas the SDM fails in reflecting this phenomenon. Furthermore, regarding the mean and standard deviation of the normalized peak IDRs, the 2DM generally performs better than the SDM, irrespective of the vertically irregular buildings with strong or stiff-and-strong lower stories [10].

4. Summary and conclusions

This study decomposed the conventional single-degree-of-freedom (SDOF) modal equations of motion for vertically irregular buildings with strong or stiff-and-strong lower stories into two-degree-of-freedom (2DOF) modal equations of motion. In addition to the 2DOF modal equations of motion, the two pushover curves simultaneously obtained from the *n*-th modal pushover analysis were used together to construct the *n*-th 2DOF modal system for the target buildings. One of the two pushover curves represents the relationship between the top displacement of the upper-structure and the base shear. The other represents the relationship

between the top displacement of the base-structure and the base shear. The two pushover curves presented in the acceleration–displacement–response spectra format fully overlap each other as the building remains elastic, whereas the two curves bifurcate after the building yields. This study showed that the 2DOF modal system is identical to the SDOF modal system for elastic buildings with the specific vertical irregularities. In addition, it was found that the more inelastic excursions a building with the specific vertical irregularities experiences, the less effective using the SDOF modal system to simulate the distinct modal responses for the upper-structure and base-structure will be. The proposed 2DOF modal system precisely overcame the stated deficiency of the SDOF modal system for buildings with the specific vertical irregularities. Through incorporating the 2DOF modal systems into the uncoupled modal response history analysis, the peak inter-story drift ratios (IDR) of four 9-story and four 20-story vertically irregular buildings, which have the lower stories stronger or stiffer-and-stronger than the upper stories, were satisfactorily estimated, compared with those estimated by adopting the SDOF modal systems. The investigation results highlight that the drastic change in the peak IDRs, over the two stories where the abrupt change in strength occurs, was poorly reflected by using the SDOF modal systems. In contrast, the 2DOF modal systems adequately captured this characteristic.

5. References

[1] Soni DP, Mistry BB (2006): Qualitative review of seismic response of vertically irregular building frames. *ISET Journal of Earthquake Technology*, *Technical Note*, **43** (4), 121-132.

[2] Chintanapakdee C, Chopra AK (2004): Seismic response of vertically irregular frames: response history and modal pushover analyses. *Journal of Structural Engineering*, ASCE, **130** (8), 1177-1185.

[3] Chopra AK, Chintanapakdee C (2004): Evaluation of modal and FEMA pushover analyses: vertically "regular" and irregular generic frames. *Earthquake Spectra*, **20** (1), 255-271.

[4] Chopra AK, Goel RK (2002): A modal pushover analysis procedure for estimating seismic demands for buildings. *Earthquake Engineering and Structural Dynamics*, **31**, 561-582.

[5] Lin JL, Tsai KC (2007): Simplified seismic analysis of asymmetric building systems. *Earthquake Engineering and Structural Dynamics*, **36**, 459-479.

[6] Chopra AK (2007): *Dynamics of Structures: Theory and Applications to Earthquake Engineering*. Prentice Hall, 3rd Edition.

[7] UBC (1994): *Uniform building code*. International Conference of Building Officials, Whittier, CA.

[8] FEMA-355C (2000): State of the art report on systems performance of steel moment frames subject to earthquake ground shaking. prepared by the SAC Joint Venture for the Federal Emergency Management Agency.

[9] Lin BZ, Chuang MC, Tsai KC (2009): Object-oriented development and application of a nonlinear structural analysis framework. *Advances in Engineering Software*, **40**, 66–82.

[10] Lin JL, Tsaur CC, Tsai KC (2019): Two-degree-of-freedom modal response history analysis of buildings with specific vertical irregularities. *Engineering Structures*, **184**, 505-523.

